Modeling and Simulation of the Central Nervous System Control with Generic Fuzzy Models

Angela Nebot
Llenguatges i Sistemes Informàtics
Universitat Politècnica de Catalunya
Mòdul C6—Campus Nord
Jordi Girona Salgado, 1-3, Barcelona 08034, Spain
angela@lsi.upc.es

Francisco Mugica
Centro de Inv. en Ciencia Aplicada y Tec. Avanzada (CICATA)
Instituto Politécnico Nacional
Legaria 694, Col.Irrigación, C.P.115000, México D.F.

François E. Cellier
Department of Electrical & Computer Engineering
University of Arizona
Tucson, AZ 85721-0104, USA

Montserrat Vallverdú
Dept. ESAII—Centre de Recerca en Eng. Biomèdica
Universitat Politècnica de Catalunya
Pau Gargallo 5, Barcelona 08028, Spain

The analysis of the human cardiovascular system by means of modeling and simulation methodologies is of relevance from a medical point of view because it allows doctors to acquire a better understanding of cardiovascular physiology, offer more accurate diagnostics, and select better suited therapies. The cardiovascular system is composed of the hemodynamical system and the central nervous system (CNS). In this work, two generic models of the CNS for patients with coronary diseases are identified by means of the fuzzy inductive reasoning (FIR) methodology. One of the models is generic only in its structure, whereas the other one is a fully generic model. It is very useful for doctors to have available a generic CNS model for a group of patients with common characteristics because this model can be used to predict the future behavior of new patients with the same characteristics.

Keywords: Inductive reasoning, fuzzy systems, central nervous system, cardiovascular system, generic models

1. Introduction

The human cardiovascular system consists of two parts, the hemodynamical system and the central nervous system (CNS). The hemodynamical system operates essentially like a hydro-mechanical pump, and consequently, its structure and functioning are well understood. This is why a considerable number of accurate quantitative hemodynamical system models can be found in the open literature [1-4]. The central nervous system is in charge of controlling the hemodynamical system. In contrast to the hemodynamical system, the functioning of the CNS is of high complexity, and the structural mechanisms responsible for the control actions are not very well known. The analysis of the regulation done by the CNS controllers to the hemodynamical system and its application to patients with coronary diseases are of high importance for the diagnosis and selection of better suited therapies.

SIMULATION, Vol. 79, Issue 11, November 2003 648-669

DOI: 10.1177/0037549703038883

Fuzzy inductive reasoning (FIR), a qualitative methodology based on fuzzy logic, is chosen in this article as the modeling and simulation tool for dealing with the CNS. Previous studies have demonstrated that the FIR methodology is capable of capturing the dynamic behavior of the CNS control for a specific patient [5, 6]. In these publications, it was shown that the FIR models synthesized were more robust and accurate than the models obtained using NARMAX and neural network (NN) inductive approaches. However, these models were obtained and validated using data from a single patient, and therefore, a deep study (with more patients) is required to confirm these preliminary results.

The main goal of this research is the identification of generic models of the CNS for a set of patients with similar characteristics. By *generic* models, we mean models that are not useful for a single patient but useful for a group of patients with common characteristics. In this way, the generic models can be used to predict the behavior of new patients who belong to that specific group.

An important effort is spent on the validation process of the generic CNS models. On one hand, the generic CNS models obtained are validated in an open loop using test data sets not used in the identification process. On the other hand, the cardiovascular system is simulated as a whole (closed loop) to prove that the generic CNS models obtained perform an accurate control to the hemodynamical system of specific patients.

To this end, two particular tasks were established. The first one is to infer a generic model of the CNS control for the set of available patients. Two different approaches were considered. On one hand, a *generic-structure* FIR model is obtained by choosing the structure of the single-patient model that performs best from a prediction point of view. In this case, the structure of the model (called *mask* in FIR nomenclature) is one and the same for all patients and is the basis of the generic model, whereas the rule base (called *behavior matrix* in FIR nomenclature) is specific for each patient. The idea behind this approach is derived from the common generalization strategy carried out by parametric modeling methodologies (i.e., NARMAX) [7]. In this case, the structure of the NARMAX models (the linear and nonlinear terms) are the same, but their parameters are specific for each patient. On the other hand, a *fully generic* FIR model is inferred from all the data obtained from the different patients. Both types of generic models inferred are validated and compared from a prediction accuracy point of view.

The second objective of the study consists of closing the loop between the hemodynamical system, modeled by means of differential equations (quantitative model), and the CNS control, modeled in terms of the FIR methodology (qualitative model). The mixed quantitative/qualitative generic model of the cardiovascular system is validated using real physiological data obtained from cardiac catheterization.

2. The Cardiovascular System

As mentioned previously, the cardiovascular system is composed of the hemodynamical and the central nervous system (CNS) subsystems. Figure 1 shows a schematic diagram of the cardiovascular system. The cardiovascular system is a dynamic complex system in which several actions must be considered: ventricle filling in and emptying out, blood flow through the entire organism, control actions made by the central nervous system, and the interaction of the cardiovascular system with other body systems.

The main task of the hemodynamical system is to ensure the continuous flow of blood in the human body to carry the oxygen and the necessary metabolic substances to the tissues, as well as to eliminate the oxidation products. The main task of the central nervous system is to control the hemodynamical system by generating the regulating signals for the blood vessels and the heart. These signals are transmitted through the sympathetic and parasympathetic nerves, producing stimuli in the corresponding organs and other body parts.

As shown in Figure 1, the CNS is considered to be composed of five controllers: *heart rate*, *myocardiac contractility*, *peripheric resistance*, *venous tone*, and *coronary resistance*. All of them are single-input/single-output (SISO) models driven by the same input variable, namely, the *carotid sinus pressure*.

The hemodynamical system has been widely studied, and its mechanisms are in compliance with the laws of fluid mechanics. The acquired knowledge of the structure and functioning of the hemodynamical system has allowed the development of fairly accurate quantitative models [1–3, 8]. These are based on models of the arterial, vein, and cardiac systems. One of the most detailed quantitative hemodynamical models was developed by Vallverdú and is reported in Vallverdú, Crexells, and Caminal [4]. In this model, the heart is composed of four chambers, modeled from the relations between pressure, volume, and elasticity variables.

Vallverdú's quantitative hemodynamical model [4] has been adopted in this study since it offers a fairly high degree of internal validity. The model is described through a set of highly nonlinear ordinary differential equations.

The functioning of the central nervous system is not fully understood, and because of that, many of the cardiovascular system models developed so far have been designed without taking into account the effects of CNS control. Quantitative models for each of the hypothesized control mechanisms have been postulated by various authors [9–11]. However, these models offer a considerably lower degree of internal validity in comparison with the models used to describe the hemodynamical system.

The use of inductive modeling techniques (e.g., FIR methodology), with flexibility for properly reflecting the input/output behavior of a system, offers an attractive alternative to the differential equation models [5, 6]. Furthermore, FIR offers a self-assessment capability that makes

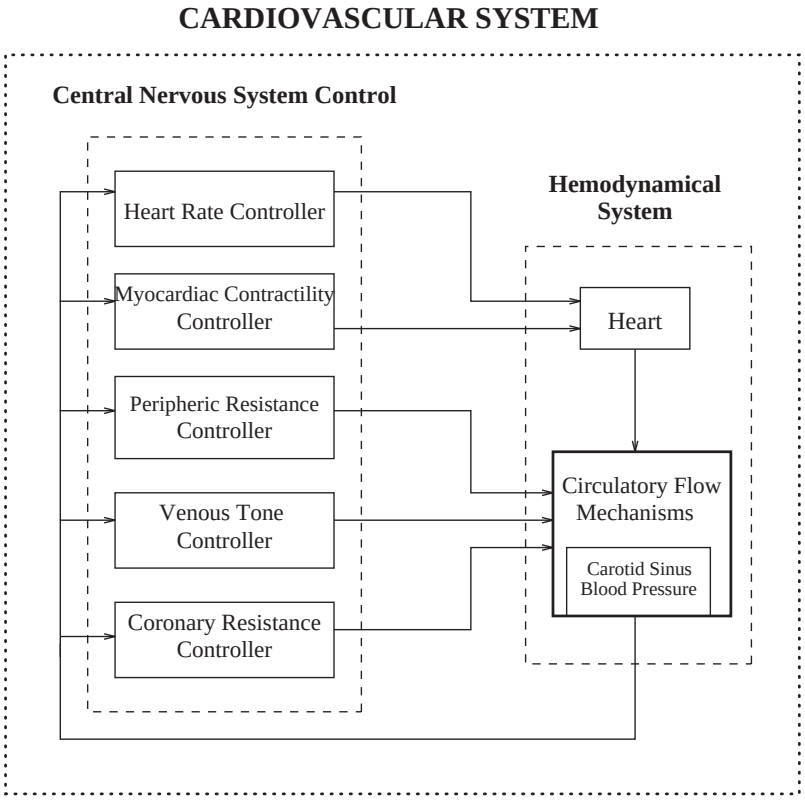

Figure 1. Simplified diagram of the cardiovascular system model

these models more robust than the differential equation models.

The identification and validation data used in the present research are the same set of signals used in Vallverdú [7], where a NARMAX model of the cardiovascular system was identified and validated. These data sets were obtained from the simulation of a differential equation model of the central nervous system that represents an enhancement of many individual previous research efforts described by various authors [1–4, 8] and is therefore one of the most complete deductive CNS descriptions currently available. The differential equation model has been tuned to represent five specific patients suffering from different percentages of coronary arterial obstruction by making the four different physiological variables—right auricular pressure, aortic pressure, coronary blood flow, and heart rate—of the simulation model agree with the measurement data taken from each patient.

3. Fuzzy Inductive Reasoning Methodology

In this section, an overview of the fuzzy inductive reasoning methodology is presented. A deep explanation of the methodology is presented in the appendix. FIR is based on the *general system problem solver* (GSPS) [12], a tool for general system analysis that allows one to study the conceptual modes of behavior of dynamical systems. FIR is a data-driven methodology based on systems behavior rather than structural knowledge. It is able to obtain good qualitative relations between the variables that compose the system and to infer future behavior of that system. It is therefore a very useful tool for modeling and simulating systems for which no previous structural knowledge is available (e.g., biomedical systems). FIR methodology is composed of four main processes—namely, *fuzzification*, *qualitative modeling*, *qualitative simulation*, and *defuzzification*.

FIR is fed with data measured from the system under study, converted into fuzzy information by means of the fuzzification function. In the fuzzification process, quantitative values are fuzzified (discretized) into a fuzzy triple, consisting of the class, the membership, and the side (cf. the appendix). The side function gives information about the position of the quantitative value with respect to the maximum of the membership function of the chosen class. It is important to notice that the same information is contained in the qualitative triple as in the quantitative value, and hence no information is lost in the fuzzification process. To convert quantitative values into qualitative ones, it is necessary to provide to the function the number of classes

into which the space is going to be discretized and the landmarks that separate neighboring classes from each other. The qualitative modeling process of the FIR methodology is responsible for finding spatial and temporal causal relations between variables and, therefore, for obtaining the best model (composed by the mask and the behavior matrix) that represents the system. The qualitative modeling process evaluates the possible masks and concludes which among them has the highest quality from the point of view of an entropy reduction measure. Then the mask is used to obtain the behavior matrix (rule base) associated with the data registered from the system. An example of a mask is presented in equation (1):

$$\begin{array}{c} {}_t\backslash^x \\ t-2\delta t \\ t-\delta t \\ t \end{array} \begin{array}{c} \begin{array}{ccc} Input1 & Input2 & Output \end{array} \\ \begin{pmatrix} 0 & -1 & 0 \\ -2 & 0 & -3 \\ -4 & 0 & +1 \end{pmatrix} \end{array}. \tag{1}$$

Negative entries in the mask are called m-inputs (mask inputs). They denote causal relations with the output (i.e., they identify those m-inputs that are most useful for extracting information about the output). The single positive entry denotes the output. The number of nonzero elements is called the *complexity* of the mask. The number of rows in the mask is called the *depth*.

In the above example, the Output at time t is said to be a function of Input2 at time $t - 2\delta t$, of Input1 at time $t - \delta t$, of the Output itself at time $t - \delta t$, and of Input1 at time t.

The mask candidate matrix (see equation (2)) describes the set of all possible masks that the qualitative modeling process needs to consider when determining the best one (i.e., the optimal mask).

$$\begin{array}{c} {}_t\backslash^x \\ t-2\delta t \\ t-\delta t \\ t \end{array} \begin{array}{c} \begin{array}{ccc} Input1 & Input2 & Output \end{array} \\ \begin{pmatrix} -1 & -1 & -1 \\ -1 & -1 & -1 \\ -1 & -1 & +1 \end{pmatrix} \end{array} \tag{2}$$

The negative elements in the mask candidate matrix represent potential causal relations with the output. If previous knowledge of the system is available—for example, if it is a priori known that some variables are not or only poorly related with the output—this information can be incorporated into the mask candidate matrix by introducing zero elements that block the investigation of a causal relation between that specific m-input and the selected output.

Once the best mask has been identified, it can be applied to the qualitative data obtained from the system, resulting in a particular rule base (behavior matrix).

Once the rule base and the mask are available, a prediction can take place using FIR's inference engine. This process is called qualitative simulation. The FIR inference engine is a specialization of the k-nearest neighbor (k-NN) rule, commonly used in pattern recognition. The adaptation of the generic k-NN rule to a variant of a five-nearest-neighbors (5-NN) method has proven very successful in the past, leading usually to good results when applied to biomedical systems [5, 13].

Defuzzification is the inverse process of fuzzification. It allows conversion of the qualitative-predicted output to quantitative values that can then be used as inputs to an external quantitative model. The reader is referred to the appendix for a more detailed understanding of the FIR methodology.

4. Generic-Structure FIR Model

This section describes how the generic-structure FIR model of the CNS is inferred from the five patients available. Before that, some general considerations need to be addressed.

As mentioned earlier, the five CNS controllers are SISO models driven by the same input variable, the *carotid sinus pressure* (see Fig. 1). The five output variables of the controller models are not directly amenable to a physiological interpretation, except for the heart rate controller variable, which is the inverse heart rate, measured in seconds between beats. The input and output signals of the CNS controllers, for all patients, are recorded with a sampling rate of 0.12 seconds from simulations of the purely differential equation model [4].

Each CNS control model is validated by using it to forecast six data sets not employed in the training process. Each one of these six test data sets, with a size of about 600 data points each, contains signals representing specific morphologies, allowing the validation of the model for different system behaviors. Data set 1 represents two consecutive Valsalva maneuvers of 10 seconds duration separated by a 2-second break, data set 2 shows two consecutive Valsalva maneuvers of 10 seconds duration separated by a 4-second break, and data set 3 exhibits two consecutive Valsalva maneuvers of 10 seconds duration separated by an 8- second break. Data set 4 shows a single Valsalva maneuver of 10 seconds duration with an intensity (pressure) increase of 50% relative to the previous three data sets. Data set 5 describes a single Valsalva maneuver of 20 seconds duration with nominal pressure. Data set 6 is called the reference data set since it represents a standardized Valsalva maneuver from which all the other variants are derived by modifying a single parameter. Figure 2 shows the six heart rate controller test data sets for patient 1.

The Valsalva maneuver, described in 1704 by Antonio de Valsalva, is a useful test in cardiology because it causes important hemodynamical changes in a short time span, can be carried out easily and painlessly by any patient, and does not have any undesirable side effects. It consists of attempting a brisk exhalation with the nose and mouth closed, blocking the passage of air and thereby provoking the increase of intrathoracic and intra-abdominal pressures.

In the modeling process, the normalized mean square error (in percentages) between the simulated output, $\hat{y}(t)$, and the system output, $y(t)$, is used to determine the

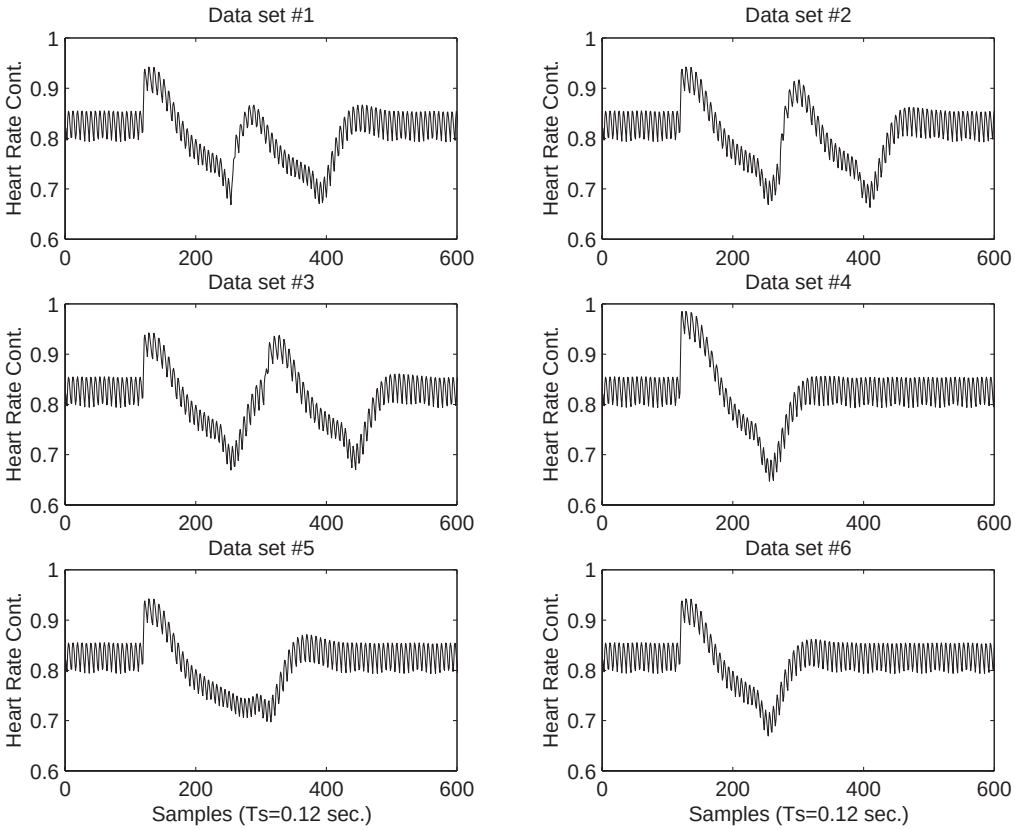

Figure 2. Heart rate controller test data sets for patient 1

validity of each of the control models. The error equation is given in (3).

$$MSE = \frac{E[(y(t) - \hat{y}(t))^2]}{y_{\text{var}}} \cdot 100\%, \tag{3}$$

where y_{var} denotes the variance of $y(t)$.

For FIR to find the best model that represents the system, the user must provide the *number of classes* into which each system variable is to be discretized, as well as the *depth* of the mask candidate matrix. Usually, both values are chosen heuristically by the modeler. However, it is necessary to take into account that the mask should cover the largest time constant of importance of the system under study [14]. Therefore, the depth can be computed by means of equation (4).

$$depth = round(\frac{\Delta t}{\delta t}) + 1, \tag{4}$$

where Δt represents the largest time constant, and δt represents the sampling rate, respectively.

If the physical system itself is available for experimentation, a Bode diagram of the system can be obtained through measurement to determine the shortest and largest time constants of concern. From there, the sampling rate can be determined as 1/2 of the shortest time constant, and the depth of the mask candidate matrix can then be determined in accordance with equation (4). However, if the physical system is not amenable to experimentation, such as in the case of biomedical systems involving humans, the modeler may have to rely on expert opinion as to what these time constants may be. In the present study, no information related to the time constants is available from the doctors. Therefore, it was decided to use the information derived from the distribution of the data (histograms) to estimate the optimal number of classes, as well as the information obtained from the study of the existence of Markov properties to determine the optimal depth of the mask candidate matrix.

Figure 3 describes the FIR process of obtaining a qualitative model of the CNS for each patient when using Markovian models and data distribution analysis to enhance the prediction capability of FIR models.

The first step is to compute the histogram of the training data for each system variable. The histogram provides information about the distribution of data helping the modeler to decide the number of classes into which the system variables are to be discretized and to determine the

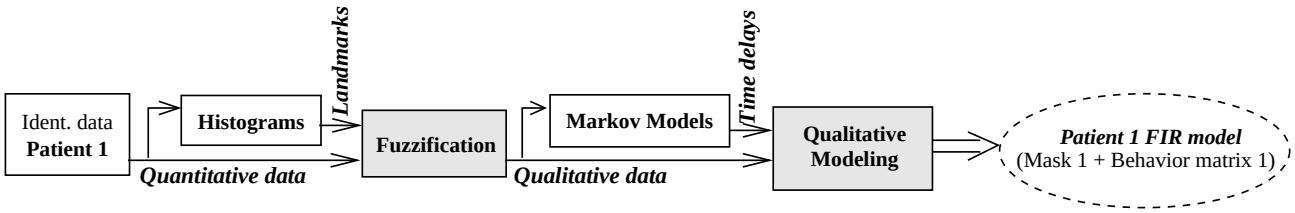

Figure 3. Qualitative identification process

landmarks (limits between classes) of each class. Once the number of classes and the landmarks have been determined, the fuzzification process of the FIR methodology can take place. How this is done will be shown in due course by means of an example.

The second step is to compute the single-dependency Markovian models of variable order that can help to identify the depth of the mask and to extract as much information as possible about the temporal relations of the input and output variables.

The information provided by this method allows the inclusion of a priori knowledge about the system into the mask candidate matrices, thus reducing their complexity and, therefore, making the search space smaller. Consequently, the time spent by the FIR qualitative modeling process to find the optimal mask is considerably reduced. However, it is important to notice that the single-dependency Markovian models provide relevant temporal relations for a single variable only and not between different variables, which would be of much interest.

Once the best mask is found, it is applied to the qualitative data obtaining a behavior matrix. Together, the *mask* and the *behavior matrix* constitute the system model.

Let us now focus on obtaining a generic-structure CNS model. The idea derives from the common generalization strategy embraced by most parametric modeling methodologies, such as NARMAX [7]. In Vallverdú [7], the structure of the NARMAX models (the linear and nonlinear terms) is identical for all patients, but their parameter values are different for each patient. In the FIR methodology, the mask can be viewed as the structure of the model, whereas the rule base (behavior matrix) can be considered specific for each patient because it is derived from its own measured data. Therefore, there is an analogy between the mask of the FIR methodology and the number and types of terms used in the NARMAX equations, as well as between behavior matrices and the parameter values.

How is the structure (mask) of the generic CNS model obtained? To identify a mask that best represents the common structure of all patients, it is decided to choose the patient- specific mask that exhibits the best performance from the prediction point of view. The mask of the patient with the lowest cumulative prediction error is selected as the generic structure for all the patients with similar characteristics. Therefore, to identify the best patient-specific mask from the prediction accuracy perspective, it becomes necessary to obtain CNS models for each of the five patients available.

To this end, specific models are obtained for each patient (5) and each controller (5), resulting in 25 different FIR models. The same inference procedure is used to obtain each of the 25 FIR models. As an example, this process is described for only one of these controllers, namely, the heart rate of patient 4.

4.1 Heart Rate Controller

As described in Figure 3, to determine the number of classes and the landmarks associated with each class, it is necessary to compute the histogram of the training data for each system variable. Figure 4 presents the histogram obtained for the carotid sinus pressure (input variable) for patient 4.

The distribution of the data defines four separate groups in a natural way. The first one corresponds to the interval [55 90]. The second, third, and fourth are associated with the intervals [90 130], [130 163], and [163 205], respectively. Consequently, the input variable for all the controllers of patient 4 was discretized into four classes (named $C1$, $C2$, $C3$, and $C4$ in Fig. 4), with landmarks as defined above. The same procedure was used to obtain the number of classes and landmarks of the output variable. In this case, the heart rate controller was discretized into three classes. With the information extracted from the histograms, the fuzzification procedure is applied for the input and output variables, obtaining a qualitative data set.

The next step is to apply the Markov property test to the input and output signals of the heart rate controller. The upper part of Figure 5 shows the result of applying a Markov test to the carotid sinus pressure (CSP: input variable). In the lower part of the same figure, the result of applying the same Markov test to the heart rate controller (HRC: output variable) is presented.

The peaks of Figure 5 represent strong temporal relations with respect to the same variable at the present time. Consequently, the lower part of Figure 5 shows that the HRC at present time is highly dependent on the values of the same signal 1, 6, 12, and 17 steps back in time. In the same way from the upper part of Figure 5, it becomes evident that the CSP signal at the present time is most

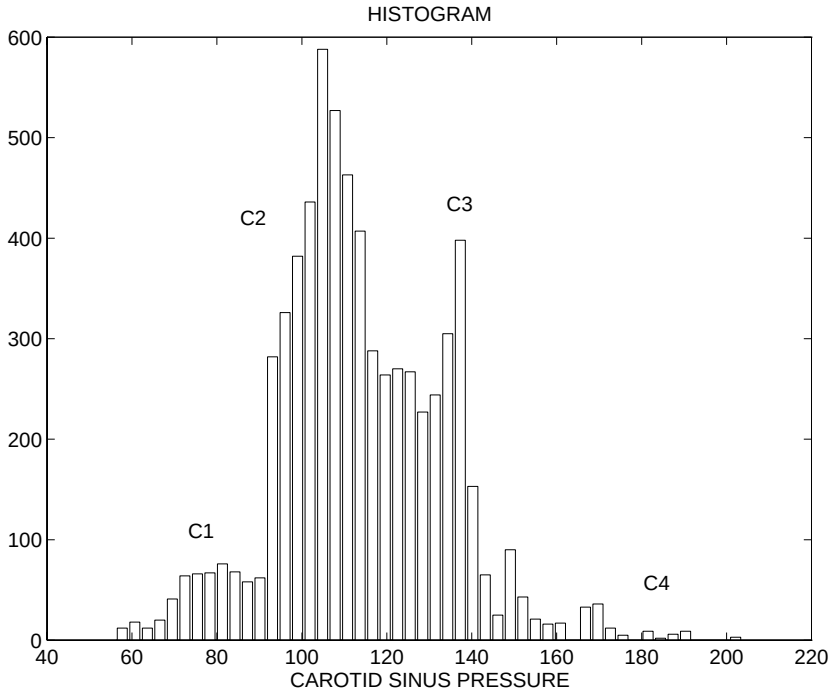

Figure 4. Histogram of the carotid sinus pressure for patient 4

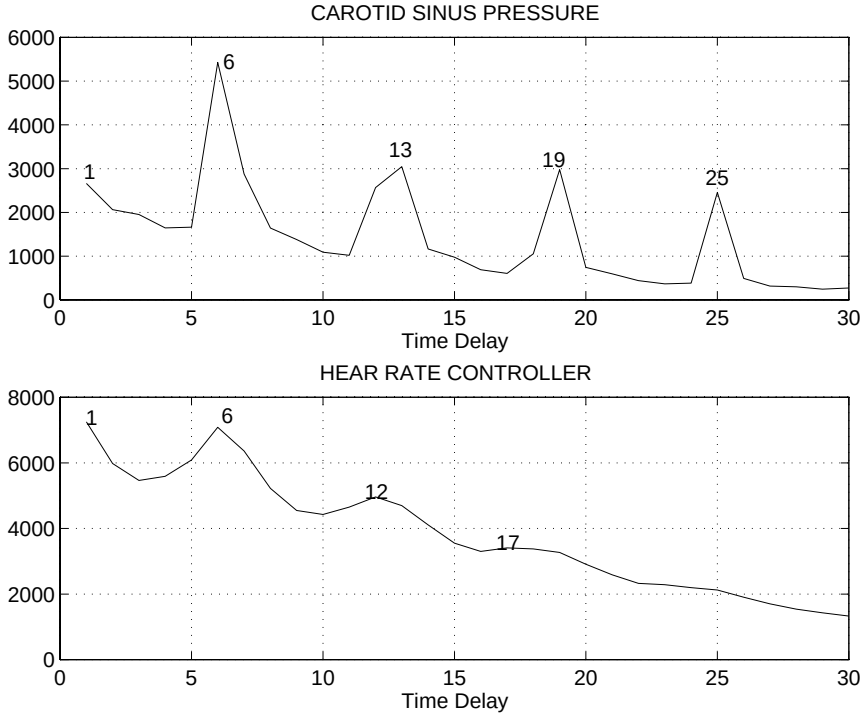

Figure 5. Single-dependency, variable-order Markovian property test applied to carotid sinus pressure (CSP) and heart rate controller (HRC) variables for patient 4

strongly dependent on the same signal 1, 6, 13, 19, and 25 steps back in time. This information was used to define the mask candidate matrix associated with the heart rate controller for patient 4 in the way described in equation (5).

$$
\begin{array}{c|cc}
t\backslash x & CSP & HRC \\
t-25\delta t & -1 & 0 \\
\vdots & \vdots & \vdots \\
t-19\delta t & -1 & 0 \\
\vdots & \vdots & \vdots \\
t-17\delta t & 0 & -1 \\
\vdots & \vdots & \vdots \\
t-13\delta t & -1 & 0 \\
t-12\delta t & 0 & -1 \\
\vdots & \vdots & \vdots \\
t-6\delta t & -1 & -1 \\
\vdots & \vdots & \vdots \\
t-\delta t & -1 & -1 \\
t & -1 & +1
\end{array}
\tag{5}
$$

The mask candidate matrix was chosen in this way to speed up the qualitative modeling process. Evidently, the proposed algorithm only picks up linear or linearizable dependencies between variables, and in some cases, it may be necessary to augment the mask candidate matrix with additional -1 entries to obtain a satisfactory model of the process.

With the mask candidate matrix available, the qualitative modeling process of the FIR methodology is used to obtain the optimal mask for the heart rate controller subsystem. The best mask obtained is presented in equation (6).

$$
\begin{array}{c|cc}
t\backslash x & CSP & HRC \\
t-25\delta t & 0 & 0 \\
\vdots & \vdots & \vdots \\
t-19\delta t & -1 & 0 \\
\vdots & \vdots & \vdots \\
t-17\delta t & 0 & -2 \\
\vdots & \vdots & \vdots \\
t-13\delta t & -3 & 0 \\
t-12\delta t & 0 & -4 \\
\vdots & \vdots & \vdots \\
t-6\delta t & -5 & -6 \\
\vdots & \vdots & \vdots \\
t-\delta t & -7 & -8 \\
t & 0 & +1
\end{array}
\tag{6}
$$

The mask of equation (6) can be interpreted as follows: the heart rate controller at the current time t depends on the values of the carotid sinus pressure at 0.12, 0.72, 1.56, and 2.28 seconds in the past and also on its own values at 0.12, 0.72, 1.44, and 2.04 seconds in the past.

The optimal mask can be written as

$$
\begin{aligned}
HRC(t) = \widetilde{f}(&CSP(t-19\delta t), \\
&HRC(t-17\delta t), CSP(t-13\delta t), \\
&HRC(t-12\delta t), CSP(t-6\delta t), \\
&HRC(t-6\delta t), CSP(t-\delta t), \\
&HRC(t-\delta t)),
\end{aligned}
\tag{7}
$$

where $\widetilde{f}$ denotes a qualitative relationship. The FIR qualitative modeling engine picked a mask of high complexity in this case, which is rather unusual in the case of a two-variable system. It indicates that the carotid sinus pressure indeed contains a lot of information about the heart rate controller variable and points to the fact that much measurement data were available to warrant the selection of a high-quality model.

The optimal mask is then applied to the qualitative data (see Fig. 13, presented later) to determine the associated behavior matrix. The heart rate controller model (mask and behavior matrix) identified for patient 4 is validated by predicting the six test data sets available for that patient and that controller by using FIR's qualitative simulation process. The average prediction error (MSE) obtained is $7.3e-5\%$, presented in the first row/fourth column of Table 1.

Figures 6 and 7 show the prediction results of two of the six test data sets (MV4 and REF, respectively) used for the validation of the model. In the upper plot of these figures, the real and the predicted output signals are plotted together. Both signals are indistinguishable due to the high accuracy of the prediction. The lower plot of those figures is included to show the prediction errors obtained (real minus predicted values) to provide an example of the amazing precision of the predictions made.

As demonstrated, the FIR model is capable of properly forecasting both the low- frequency and the high-frequency behaviors of these signals. The MSE (in percentages) for the MV4 test data set is $2.6e-6\%$, whereas this error is 0.0321% for the REF test data set.

The same procedure was used to infer optimal models of the other controllers for the same patient and all CNS controller models for the remaining patients. The average MSE errors (in percentages) obtained for the six test data sets for all controllers and patients are summarized in Table 1. Each column corresponds to one patient, and each row contains the average MSE error obtained for the six validation data sets for each particular controller.

The results presented in Table 1 show that the FIR approach is indeed capable of capturing in a reliable way the dynamic behavior of the system under study for all patients. The average errors obtained for the five controllers of the five patients are very low. It is interesting to notice that the venous tone controller model for patient 5 does not perform as accurately as the other models. However, the

Table 1. Average MSE errors of the HRC, PRC, MCC, VTC, and CRC FIR models for the five patients (in percentages)

	Patient 1	Patient 2	Patient 3	Patient 4	Patient 5
HRC	5.0e-4	4.6e-3	1.0e-3	7.3e-5	7.0e-4
PRC	9.0e-4	3.0e-4	4.9e-5	7.0e-4	3.3e-4
MCC	2.6e-3	2.0e-3	1.0e-4	7.6e-6	1.4e-4
VTC	7.3e-3	3.0e-4	4.7e-3	7.9e-4	4.9
CRC	8.0e-4	2.0e-4	6.8e-3	3.0e-4	4.4e-5

Note. MSE = mean square error; HRC = heart rate controller; PRC = peripheric resistance controller; MCC = myocardiac contractility controller; VTC = venous tone controller; CRC = coronary resistance controller; FIR = fuzzy inductive reasoning.

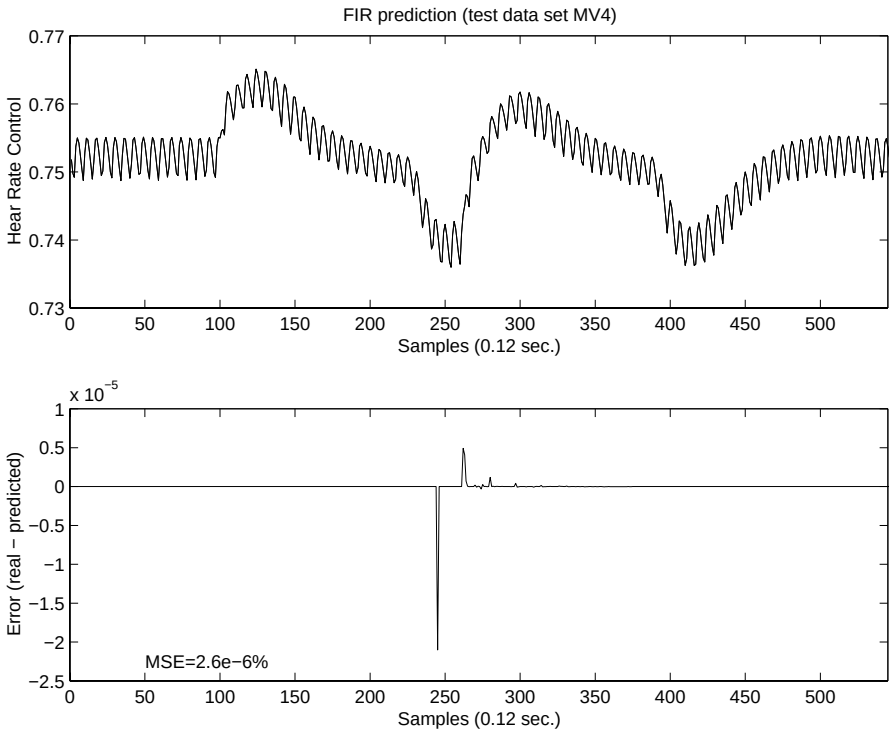

Figure 6. Heart rate control of patient 4: Prediction MV4 test data set

error obtained in that case is 4.9%, which is still very low if compared with the error obtained when other modeling techniques, such as NARMAX [5] or either time-delayed or recurrent neural networks [6], are used.

Once all CNS controllers for each of the five available patient data sets are modeled, the process of obtaining a generic-structure model can take place. The identification of a generic-structure model for a given controller is done by choosing the mask that is associated with the lowest MSE error from the set of masks of all the patients that represent the specific controller. As illustrated in Figure 8, the mask of patient 1 (mask 1) is used together with the behavior matrices of every patient to predict the test data sets associated with that patient for a given controller. From the errors obtained for each patient (MSE i), the average error that represents the prediction performance of that mask is computed. The same procedure is done for the masks of patients 2, 3, 4, and 5. Finally, the mask of the patient that exhibits the lowest average error is the mask chosen to represent generically the structure of that controller.

Equation (8) describes the chosen mask for the heart rate controller. From the computed histograms, it was decided to discretize the input variable into four classes, whereas the output variable was discretized into three classes.

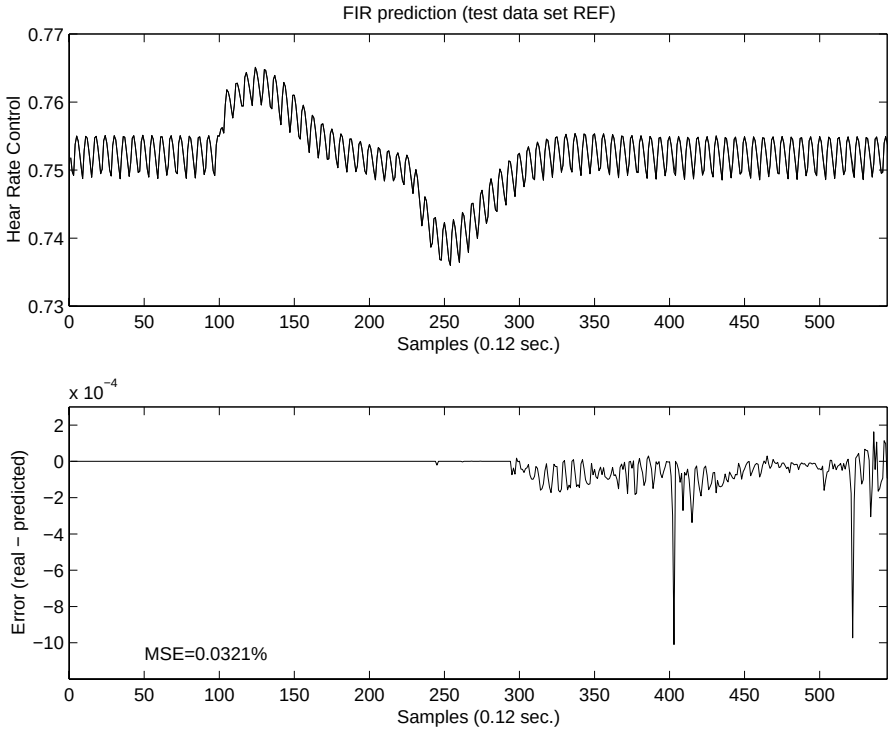

Figure 7. Heart rate control of patient 4: Prediction REF test data set

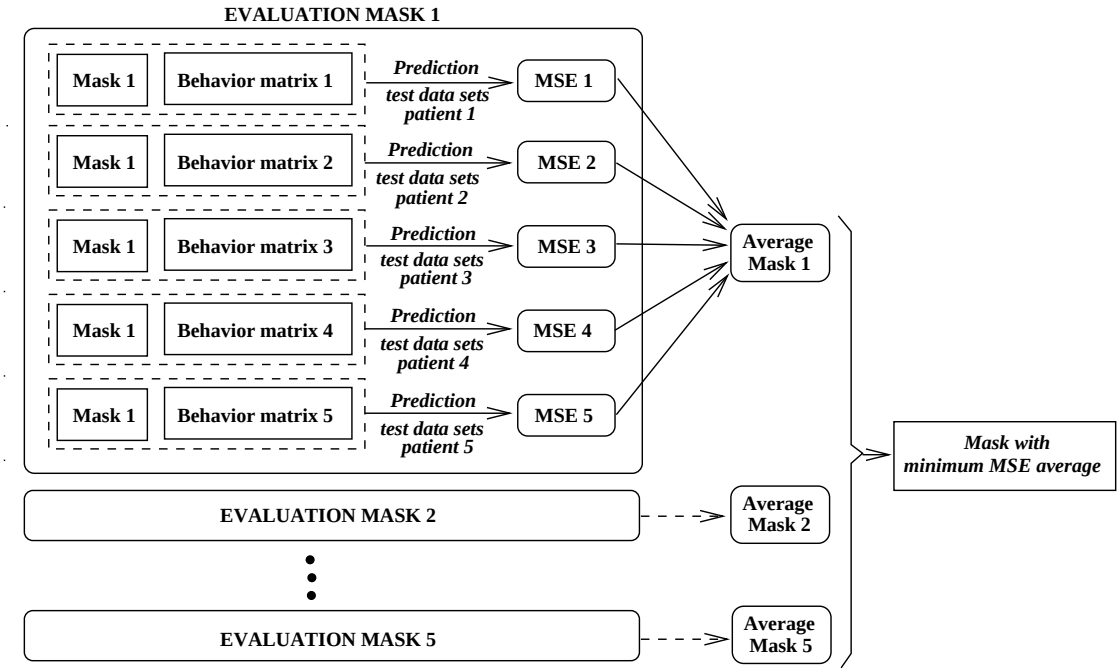

Figure 8. Identification process of a *generic-structure* mask of the central nervous system (CNS) control

$$
\begin{array}{c} {}_t\backslash^x \\ t-13\delta t \\ \vdots \\ t-7\delta t \\ \vdots \\ t-5\delta t \\ \vdots \\ t-\delta t \\ t \end{array}
\begin{array}{c} CSP \\ \begin{pmatrix} -1 \\ \vdots \\ -3 \\ \vdots \\ 0 \\ \vdots \\ -5 \\ 0 \end{pmatrix} \end{array}
\begin{array}{c} HRC \\ \begin{pmatrix} -2 \\ \vdots \\ 0 \\ \vdots \\ -4 \\ \vdots \\ -6 \\ +1 \end{pmatrix} \end{array}
\tag{8}
$$

The mask chosen in equation (8) is now used to obtain the specific behavior matrices for each patient (see the appendix). Once the generic mask and the behavior matrices are available, the different test data sets of all five patients are predicted. Notice that the structure of the model (the mask) is identical in all predictions, whereas the behavior matrix is specific for each patient. Therefore, the generic model obtained is not fully generic but generic in its structure only. The procedure of identifying a generic HRC model is fully applicable to the other CNS controllers. The peripheric resistance controller (PRC), myocardiac contractility controller (MCC), and venous tone controller (VTC) variables were also fuzzified into four classes, whereas the coronary resistance controller (CRC) variable was discretized into three classes. Equations (9) through (12) describe the best masks identified by the FIR representing the optimal generic structure of the PRC, MCC, VTC, and CRC controllers, respectively.

$$
\begin{array}{c} {}_t\backslash^x \\ t-16\delta t \\ \vdots \\ t-8\delta t \\ \vdots \\ t-6\delta t \\ \vdots \\ t-2\delta t \\ t-\delta t \\ t \end{array}
\begin{array}{c} CSP \\ \begin{pmatrix} -1 \\ \vdots \\ -2 \\ \vdots \\ 0 \\ \vdots \\ 0 \\ -5 \\ 0 \end{pmatrix} \end{array}
\begin{array}{c} PRC \\ \begin{pmatrix} 0 \\ \vdots \\ 0 \\ \vdots \\ -3 \\ \vdots \\ -4 \\ -6 \\ +1 \end{pmatrix} \end{array}
\tag{9}
$$

$$
\begin{array}{c} {}_t\backslash^x \\ t-13\delta t \\ t-12\delta t \\ \vdots \\ t-7\delta t \\ \vdots \\ t-\delta t \\ t \end{array}
\begin{array}{c} CSP \\ \begin{pmatrix} -1 \\ 0 \\ \vdots \\ -3 \\ \vdots \\ -5 \\ 0 \end{pmatrix} \end{array}
\begin{array}{c} MCC \\ \begin{pmatrix} 0 \\ -2 \\ \vdots \\ -4 \\ \vdots \\ -6 \\ +1 \end{pmatrix} \end{array}
\tag{10}
$$

$$
\begin{array}{c} {}_t\backslash^x \\ t-14\delta t \\ \vdots \\ t-7\delta t \\ t-6\delta t \\ \vdots \\ t-\delta t \\ t \end{array}
\begin{array}{c} CSP \\ \begin{pmatrix} -1 \\ \vdots \\ -2 \\ 0 \\ \vdots \\ -4 \\ 0 \end{pmatrix} \end{array}
\begin{array}{c} VTC \\ \begin{pmatrix} 0 \\ \vdots \\ 0 \\ -3 \\ \vdots \\ -5 \\ +1 \end{pmatrix} \end{array}
\tag{11}
$$

$$
\begin{array}{c} {}_t\backslash^x \\ t-16\delta t \\ \vdots \\ t-10\delta t \\ \vdots \\ t-8\delta t \\ \vdots \\ t-2\delta t \\ t-\delta t \\ t \end{array}
\begin{array}{c} CSP \\ \begin{pmatrix} -1 \\ \vdots \\ 0 \\ \vdots \\ -3 \\ \vdots \\ 0 \\ -5 \\ 0 \end{pmatrix} \end{array}
\begin{array}{c} CRC \\ \begin{pmatrix} 0 \\ \vdots \\ -2 \\ \vdots \\ 0 \\ \vdots \\ -4 \\ -6 \\ +1 \end{pmatrix} \end{array}
\tag{12}
$$

The generic structures (masks) of these controllers are used to obtain the patient-specific behavior matrices. The generic structure models are then used to predict the test data sets of all five patients.

The results obtained are summarized in Table 2. Each row contains the average error of the 6 test data sets associated with one specific patient for each CNS controller. The last row shows the global average errors of the 30 test data sets for each controller. It can be observed that the average errors for all the controllers are lower than $2.0e-3\%$, an impressively good result. Therefore, the generic-structure models identified for each controller capture in a reliable way the common behavior of this set of patients. The next step is to study the feasibility of obtaining a reliable fully generic model of the CNS.

5. Fully Generic FIR Model

Encouraged by the good results obtained when forecasting using a generic- structure CNS model, it was decided to go a step further and try to identify a fully generic CNS model. The same five patients used in the previous section are also the subjects of this study. For each of the five controllers, 35,000 data points (7000 for each patient) are used in the identification process. The generic models are validated by forecasting the 30 test data sets available for each controller (6 test data sets for patient and controller).

Figure 9 describes the process of obtaining a fully generic model of the CNS control. The identification data used for inferring the generic model of a specific controller are obtained by merging the individual identification data streams of all patients. However, it is necessary to be

Table 2. Average MSE errors of the HRC, PRC, MCC, VTC, and CRC *generic-structure* models induced by FIR (in percentages)

	HRC	PRC	MCC	VTC	CRC
Test patient 1	1.9e-5	6.8e-7	9.5e-4	4.2e-3	3.5e-4
Test patient 2	1.8e-5	6.0e-5	1.95e-4	3.3e-4	1.7e-5
Test patient 3	9.9e-4	4.6e-5	5.0e-5	2.6e-4	1.6e-5
Test patient 4	4.5e-5	2.6e-8	1.6e-10	2.7e-4	9.1e-6
Test patient 5	1.3e-4	3.3e-4	7.3e-8	1.3e-3	4.4e-5
Average error	2.4e-4	8.7e-5	2.4e-4	1.3e-3	8.7e-5

Note. MSE = mean square error; HRC = heart rate controller; PRC = peripheric resistance controller; MCC = myocardiac contractility controller; VTC = venous tone controller; CRC = coronary resistance controller; FIR = fuzzy inductive reasoning.

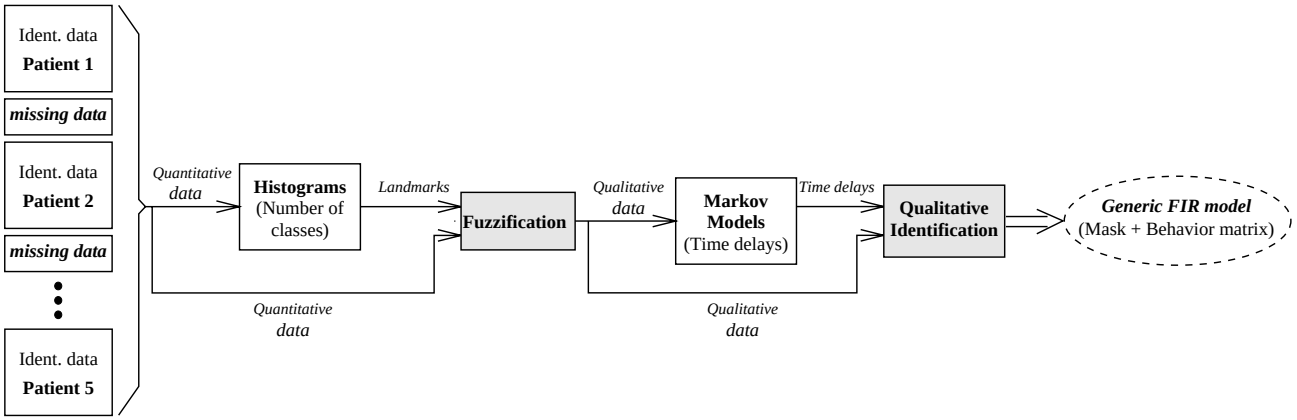

Figure 9. Identification process of a *fully generic* model of the central nervous system (CNS) control

cautious because if the data stemming from one patient are placed immediately adjacent to the data stemming from another patient, fake causal relationships would be created at the seam of the two data streams, causing a severe degradation of the forecasting power of the derived FIR model. Therefore, it is necessary to add gaps of *missing data* between neighboring data streams stemming from different patients. This is not a problem for the FIR methodology, which is able to deal with missing data records.

At this point, a data set of the available 35,000 data records padded by gaps of missing data is ready to be used for the identification of a fully generic model of one of the five CNS controllers. The quantitative data are converted to qualitative data by means of the FIR fuzzification process. As explained before, in this conversion, it is necessary to provide the number of classes into which the space is going to be discretized. To this end, the histogram of the training data is computed for each system variable, as was already done in the identification of single-patient CNS models. Once the landmarks and the training data set are available, the fuzzification function converts the quantitative data into fuzzy triples. The next step is the identification of the generic model by means of the qualitative modeling process of the FIR methodology. A prestudy of the data, based on single-dependency Markovian models of variable order, is also done in this case.

The procedure just described and illustrated in Figure 9 is used for inferring the fully generic FIR models of the five controllers that compose the CNS (i.e., HRC, PRC, MCC, VTC, and CRC). Equation (13) describes the best mask obtained by the qualitative modeling function of FIR that represents the heart rate controller. From the histograms computed for each system variable, it was decided to fuzzify the carotid sinus pressure (input variable) into three classes, whereas the heart rate control signal (output variable) was discretized into four classes.

$$
\begin{array}{c|cc}
{}_t\backslash^x & CSP & HRC \\
t-7\delta t & -1 & -2 \\
t-6\delta t & 0 & -3 \\
\vdots & \vdots & \vdots \\
t-\delta t & -4 & -5 \\
t & 0 & +1
\end{array}
\tag{13}
$$

Equation (14) describes the best mask inferred by FIR that represents the peripheric resistance controller. The histogram computed for the output variable suggested discretizing it into six classes.

$$
\begin{array}{c|cc}
t\backslash x & CSP & PRC \\
t-15\delta t & -1 & 0 \\
\vdots & \vdots & \vdots \\
t-13\delta t & 0 & -2 \\
\vdots & \vdots & \vdots \\
t-6\delta t & -3 & 0 \\
\vdots & \vdots & \vdots \\
t-\delta t & -4 & 0 \\
t & 0 & +1
\end{array}
\tag{14}
$$

Equations (15) through (17) represent the best masks obtained for the myocardiac contractility, venous tone, and coronary resistance controllers, respectively. The histograms computed for the three output variables suggested classifying each of them into five classes.

$$
\begin{array}{c|cc}
t\backslash x & CSP & MCC \\
t-13\delta t & -1 & 0 \\
\vdots & \vdots & \vdots \\
t-\delta t & -2 & -3 \\
t & 0 & +1
\end{array}
\tag{15}
$$

$$
\begin{array}{c|cc}
t\backslash x & CSP & VTC \\
t-15\delta t & -1 & 0 \\
\vdots & \vdots & \vdots \\
t-6\delta t & -2 & 0 \\
\vdots & \vdots & \vdots \\
t-\delta t & -3 & -4 \\
t & 0 & +1
\end{array}
\tag{16}
$$

$$
\begin{array}{c|cc}
t\backslash x & CSP & CRC \\
t-16\delta t & -1 & 0 \\
t-15\delta t & -2 & 0 \\
\vdots & \vdots & \vdots \\
t-6\delta t & -3 & 0 \\
\vdots & \vdots & \vdots \\
t-3\delta t & 0 & -4 \\
\vdots & \vdots & \vdots \\
t-\delta t & -5 & 0 \\
t & 0 & +1
\end{array}
\tag{17}
$$

These masks are then used to obtain the behavior matrices (rule bases) for each controller. As mentioned earlier, each of the five fully generic FIR models identified is validated by forecasting 30 different data sets not used in the identification process that represent specific morphologies. The MSE errors (see equation (3)) obtained for each general controller are presented in Table 3. The columns and rows of this table are the same as in Table 2. It can be observed that the average errors for all controllers are below 2.5%. These results are very good if we take into account that the five models inferred are completely generic and have been validated with test data sets stemming from different patients. The MCC, VTC, and CRC models behave very well for all patients, with associated errors of less than 1%. This is not the case for the HRC and PRC models. It is clear that the HRC model is able to predict more accurately the behavior of patients 4 and 5, whereas the PRC model predicts more accurately patients 1 and 5. However, the biggest errors obtained are still below 6%, a very remarkable result in comparison with the errors obtained when using other modeling methodologies such are NARMAX [7] or neural networks [15].

The results obtained when the generic-structure model identification process is used are much better than the ones obtained by means of the fully generic CNS controller model. However, the generalization power of the generic-structure models, which have a component that is directly associated with a specific patient, is lower than the generalization achieved through the fully generic models.

The second objective of the study consists of closing the loop of the cardiovascular system to validate the overall model using real physiological data. The next section describes this work in detail.

6. The Cardiovascular Closed-Loop System

In this section, the loop between the hemodynamical system, modeled by means of differential equations, and the central nervous system control, modeled in terms of inductive modeling techniques, is closed (see Fig. 1). The complex behavior of the overall cardiovascular system is now studied.

Real physiological data obtained from cardiac catheterization are used for this study. These data were obtained from the hemodynamical division of the Hospital de la Santa Creu i de Sant Pau in Barcelona. The data stem from patients with coronary arterial obstruction of at least 70%. The measured physiological variables are as follows: right auricular pressure, $P_{AD}(t)$; aortic pressure, $P_A(t)$; coronary blood flow, $F_C(t)$; and heart rate, $HR(t)$. The physiological variables were recorded during all five phases of the Valsalva maneuver.

From the trajectories of the right auricular pressure, aortic pressure, coronary blood flow, and heart rate, mean values were computed for each of the five phases of the maneuver. P_{ADM} denotes the average right auricular pressure during a given phase, P_{AM} stands for the mean aortic pressure, F_{CM} is the average coronary blood flow, and HR_M signifies the average heart rate during any one of the phases.

The measurement results obtained through cardiac catheterization for all five patients are summarized in

Table 3. Average MSE errors of the HRC, PRC, MCC, VTC, and CRC *fully generic* controller models inferred by FIR

	HRC	PRC	MCC	VTC	CRC
Test patient 1	1.58	0.10	0.17	0.22	0.15
Test patient 2	3.51	5.95	0.08	0.05	0.03
Test patient 3	2.70	3.45	0.25	0.12	0.08
Test patient 4	0.02	2.30	0.10	0.03	0.39
Test patient 5	0.05	0.17	0.14	3.50	0.05
Average error	1.57	2.39	0.15	0.78	0.14

Note. MSE = mean square error; HRC = heart rate controller; PRC = peripheric resistance controller; MCC = myocardiac contractility controller; VTC = venous tone controller; CRC = coronary resistance controller; FIR = fuzzy inductive reasoning.

Table 4. Measurement results obtained through cardiac catheterization for the five patients studied

		Patient 1	Patient 2	Patient 3	Patient 4	Patient 5
P_{ADM}	Pre-V	2	4	4	3	5
	II	54	38	40	45	38
	IV	2	5	4	3	5
P_{AM}	Pre-V	84	107	107	113	119
	II	104	99	107	117	113
	IV	86	119	107	116	125
F_{CM}	Pre-V	112	123	148	123	113
	II	89	106	82	81	87
	IV	126	118	147	128	121
HR_M	Pre-V	70	77	73	80	72
	II	75	82	78	83	75
	IV	66	70	73	78	70

Table 4. Only the mean values computed for the pre-Valsalva phase, Valsalva phase II, and Valsalva phase IV are shown in the table because these are the most significant data from a medical point of view.

The mean values presented in Table 4 were obtained from real measurements. They will subsequently be used as reference values in the model validation process. For a model to pass the acceptance test, none of the four key variables—that is, average right auricular pressure (P_{ADM}), mean aortic pressure (P_{AM}), mean coronary blood flow (F_{CM}), and average heart rate (HR_m)—may deviate from the reference values by more than $\pm 10\%$ during any of the three key phases of the Valsalva maneuver.

At this point, the question to be raised is whether a mixed model of the cardiovascular system—whereby the hemodynamical subsystem is described by means of differential equations, and the CNS control is described using a FIR model—generates results inside the $\pm 10\%$ error margin that is permitted and can therefore be considered a valid model.

The differential equation model of the hemodynamical system was implemented using the advanced continuous simulation language (ACSL) [16], a convenient software tool for the description of ordinary differential equation-based state-space models. A simplified scheme of the simulation structure is shown in Figure 10.

The hemodynamical system, modeled and simulated in a strictly quantitative fashion, is implemented in full within ACSL. Its differential equations are implemented as a continuous process to be integrated across time using one of the standard integration algorithms offered by ACSL. The CNS control, on the other hand, is implemented inside the ACSL program as a discrete process to be executed once every 0.12 seconds.

The simulation process operates in the following way. The hemodynamical system generates a continuous-time trajectory representing the *carotid sinus pressure* (CSP). This variable is sampled by the discrete process once every 0.12 seconds and is immediately being fuzzified into three qualitative classes using the FIR fuzzification engine that is coupled to the ACSL through an interface routine. The discrete process then calls five times on the FIR qualitative simulation routine to predict qualitative values of the five controller outputs. These five qualitative triples are then defuzzified into quantitative (real-valued) controller outputs using the FIR defuzzification engine. The defuzzified signals are then made available to the hemodynamical system for use within the differential equation model.

Both the generic-structure and the fully generic CNS controller models were used to simulate the overall cardiovascular system. The simulation results obtained from the mixed quantitative/qualitative cardiovascular system

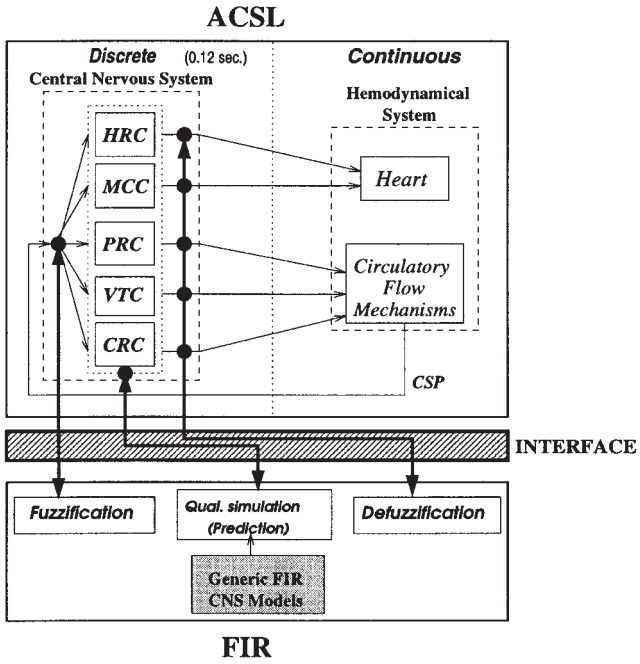

Figure 10. Schematic showing the structure of the cardiovascular system simulation program

model using generic-structure and fully generic CNS-FIR models are presented in Tables 5 and 6, respectively. The positive and negative values (in parentheses) in the tables indicate the deviations from the data obtained through cardiac catheterization.

Analyzing the results of the mixed cardiovascular system model with the generic-structure CNS control (Table 5), it is found that the largest negative relative deviations from the measurement values are -1% for patient 1, -4% for patients 2 and 3, -3% for patient 4, and -2% for patient 5. The largest positive relative deviations are $+2\%$ for patient 1, $+4\%$ for patient 2, $+2\%$ for patient 3, $+4\%$ for patient 4, and $+2\%$ for patient 5. Thus, all the indicators are within the requested $\pm 10\%$ margin, and in accordance with the requirements, this generic model is to be accepted as a valid representation of reality. The average relative deviations from the measurement values are 0.83% for patient 1, 2% for patient 2, 1.42% for patient 3, 1.25% for patient 4, and 1% for patient 5.

Performing the same analysis for the mixed cardiovascular system model with fully generic CNS control (Table 6), it can be seen that the largest negative relative deviations from the measurement values are -2% for patient 1, -4% for patients 2 and 3, and -6% for patients 4 and 5. The largest positive relative deviations are $+3\%$ for patient 1, $+6\%$ for patients 2 and 3, $+4\%$ for patient 4, and $+3\%$ for patient 5. Hence, all the indicators are again within the requested $\pm 10\%$ margin; therefore, the fully generic model is to be accepted as a valid representation of reality for the task at hand. The average relative deviations from the measurement values are 1.41% for patient 1, 2.83% for patient 2, 2.17% for patient 3, 1.83% for patient 4, and 2.25% for patient 5.

Clearly, the mixed cardiovascular system model with generic-structure CNS control shows better results than the model that includes a fully generic CNS control model. The average relative deviations are lower for all patients, and the largest negative and positive deviations, in absolute terms, are also lower (-6% vs. -4% and $+6\%$ vs. $+4\%$). Therefore, it can be concluded that the mixed cardiovascular system model, composed of a differential equation model that represents the hemodynamical system and a generic- structure FIR model representing the central nervous system control, is the overall model that better fits the real system. However, both mixed cardiovascular system models are considered acceptable from a medical point of view.

7. Conclusions

This article deals with the human cardiovascular system, which is composed of the hemodynamical and the central nervous subsystems. The modeling and simulation of the overall cardiovascular system is of great importance in the medical domain because it allows, among other things, one to acquire a deeper knowledge of the cardiovascular

Table 5. Results obtained from the mixed cardiovascular system with a *generic-structure* central nervous system (CNS) model

		Patient 1	Patient 2	Patient 3	Patient 4	Patient 5
P_{ADM}	Pre-V	2	4	4	3	5
	II	$56_{(+2)}$	38	40	45	38
	IV	2	5	4	3	5
P_{AM}	Pre-V	84	$110_{(+3)}$	$103_{(-4)}$	$117_{(+4)}$	$117_{(-2)}$
	II	$103_{(-1)}$	$101_{(+2)}$	$105_{(-2)}$	$118_{(+1)}$	$114_{(+1)}$
	IV	$88_{(+2)}$	119	$109_{(+2)}$	116	$124_{(-1)}$
F_{CM}	Pre-V	$113_{(+1)}$	$119_{(-4)}$	$144_{(-4)}$	$120_{(-3)}$	$111_{(-2)}$
	II	89	$110_{(+4)}$	$84_{(+2)}$	$83_{(+2)}$	$88_{(+1)}$
	IV	$127_{(+1)}$	$122_{(+4)}$	147	$130_{(+2)}$	$122_{(+1)}$
HR_M	Pre-V	70	$73_{(-4)}$	$75_{(+2)}$	80	$73_{(+1)}$
	II	$76_{(+1)}$	$80_{(-2)}$	$77_{(-1)}$	$81_{(- 2)}$	$74_{(-1)}$
	IV	$68_{(+2)}$	$71_{(+1)}$	73	$79_{(+1)}$	$72_{(+2)}$

Table 6. Results obtained from the mixed cardiovascular system with the *fully generic* central nervous system (CNS) model

		Patient 1	Patient 2	Patient 3	Patient 4	Patient 5
P_{ADM}	Pre-V	2	4	4	3	5
	II	$57_{(+3)}$	$40_{(+2)}$	$38_{(-2)}$	45	38
	IV	2	5	4	3	$4_{(-1)}$
P_{AM}	Pre-V	$83_{(-1)}$	$111_{(+4)}$	$113_{(+6)}$	$110_{(-3)}$	$116_{(-3)}$
	II	104	$104_{(+5)}$	107	$116_{(-1)}$	$111_{(-2)}$
	IV	$85_{(-1)}$	$117_{(-2)}$	107	$115_{(-1)}$	$119_{(-6)}$
F_{CM}	Pre-V	$113_{(+1)}$	$119_{(-4)}$	$152_{(+4)}$	$126_{(+3)}$	$109_{(-4)}$
	II	$92_{(+3)}$	$108_{(+2)}$	$87_{(+5)}$	$85_{(+4)}$	$84_{(+3)}$
	IV	$125_{(-1)}$	$124_{(+6)}$	$143_{(-4)}$	$122_{(-6)}$	$117_{(-4)}$
HR_M	Pre-V	$73_{(+3)}$	$74_{(-3)}$	73	$81_{(+1)}$	72
	II	$73_{(-2)}$	$78_{(-4)}$	$74_{(-4)}$	$82_{(- 1)}$	$71_{(-4)}$
	IV	$68_{(+2)}$	$72_{(+2)}$	$74_{(+1)}$	$80_{(+2)}$	70

physiology and furthers a better understanding of the control of the CNS over the hemodynamical system.

The work presented in this study is oriented toward the identification of a generic CNS model for patients with coronary arterial obstruction of at least 70%. Data stemming from five different patients were used to preform the study.

Two different approaches were used to infer a generic model of the CNS control. On one hand, a *generic-structure* FIR model was proposed. In this approach, the structure of each controller model is identical for all patients, whereas the rule base is specific for each patient. On the other hand, a *fully generic* FIR model was identified. Both types of generic models were validated predicting six test data sets available for each of the patients who had not been used in the modeling process. The prediction errors obtained when using the fully generic CNS models are larger than the ones obtained using the generic-structure CNS models. This is reasonable since the generalization power of the generic-structure model, having one component that is directly associated with a specific patient, is lower than the generalization achieved from the fully generic model. The errors obtained with both generic models are significantly lower than the errors obtained when using other methodologies such are NARMAX [7] or neural networks [15].

The final goal of the study consisted of closing the loop between the hemodynamical system, modeled by means of differential equations, and the CNS control, modeled in terms of the FIR methodology. The overall cardiovascular system model was validated using real physiological data obtained from cardiac catheterization from the five patients under study. Two complete cardiovascular system models were tested, one containing the generic- structure CNS models and the other incorporating the fully generic CNS models. From the validation of both models, it can be concluded that the cardiovascular system model, composed of a differential equation model representing the hemodynamical system and a set of generic-structure FIR models representing the central nervous system, is the one that better fits the real cardiovascular system. However, both

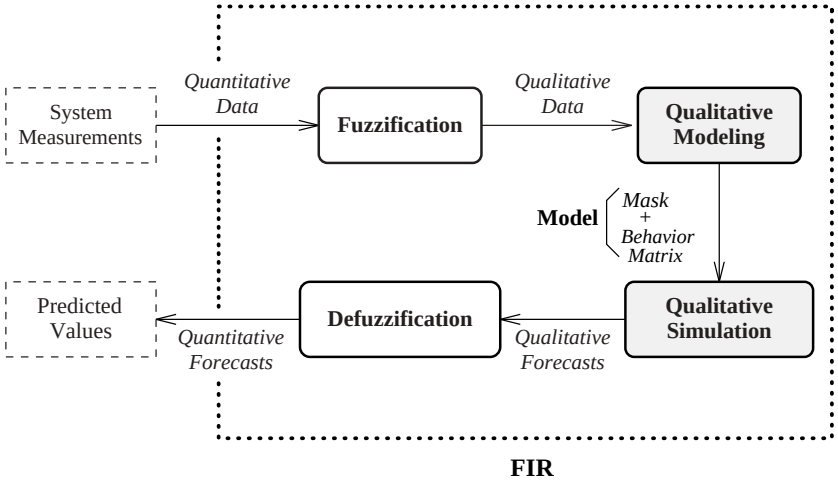

Figure 11. Schematic representation of the four primary tasks of the fuzzy inductive reasoning (FIR) methodology

mixed cardiovascular system models are considered acceptable from a medical point of view.

8. Appendix

8.1 Basics of Fuzzy Inductive Reasoning Methodology

Figure 11 shows the four main tasks of the FIR methodology in a schematic way—namely, *fuzzification*, *qualitative modeling*, *qualitative simulation*, and *defuzzification*.

The fuzzy inductive reasoner is fed with data that are measured from the system under study. These are usually quantitative—that is, real-valued, time-stamped data, such as blood pressure, body temperature, and so forth. However, FIR bases its decisions on qualitative (i.e., discretized) data. Consequently, the measurement data must first be converted from quantitative to qualitative data streams. In order not to lose information in this process, the discretization is done in a fuzzy, not crisp, sense. In Figure 11, this process is called *fuzzification*.

The predictions made by the qualitative simulation engine of FIR are qualitative predictions. It may be desirable to use these predictions subsequently as driving functions (inputs) to a quantitative model. To this end, the qualitative predictions need to be converted back to quantitative data streams. This is accomplished by the *defuzzification* engine shown in Figure 11.

The four engines that comprise the FIR methodology are described in more detail in the subsequent sections of this appendix.

8.2 Fuzzification

The fuzzification process converts quantitative values into qualitative triples. The first element of the triple is the *class value*, the second element is the *fuzzy membership value*, and the third element is the *side value*. The class value represents a coarse discretization of the original real-valued variable. The fuzzy membership value denotes the level of confidence expressed in the class value chosen to represent a particular quantitative value. Finally, the side value indicates whether the quantitative value is to the left or to the right of the peak value of the associated membership function. The side value, which is a specialty of the FIR technique since it is not commonly used in fuzzy logic, is responsible for preserving, in the qualitative triple, the complete knowledge that had been contained in the original quantitative value. Figure 12 illustrates the process of fuzzification by means of an example. A temperature of 23°C would hence be fuzzified into the class *normal* with a side value of *right* and a fuzzy membership value of 0.89.

In the current implementation of the FIR methodology, in the form of a Matlab [17] toolbox, class values are represented by positive integers—for example, in the above temperature example, by the numbers 1 representing *cold*, 2 denoting *fresh*, 3 symbolizing *normal*, 4 standing for *warm*, and 5 mapping *hot*. Similarly, the side values are implemented as -1 meaning *left*, 0 representing *center*, and +1 corresponding to *right*.

8.3 Qualitative Modeling

The qualitative behavior is stored in a *qualitative data model*. It consists of three matrices of identical sizes—one containing the class values, the second storing the membership information, and the third recording the side values. Each column represents one of the observed variables, and each row denotes one time point (i.e., one recording of all variables) or one recorded state.

In the process of modeling, it is desired to discover finite automata relations among the class values that make

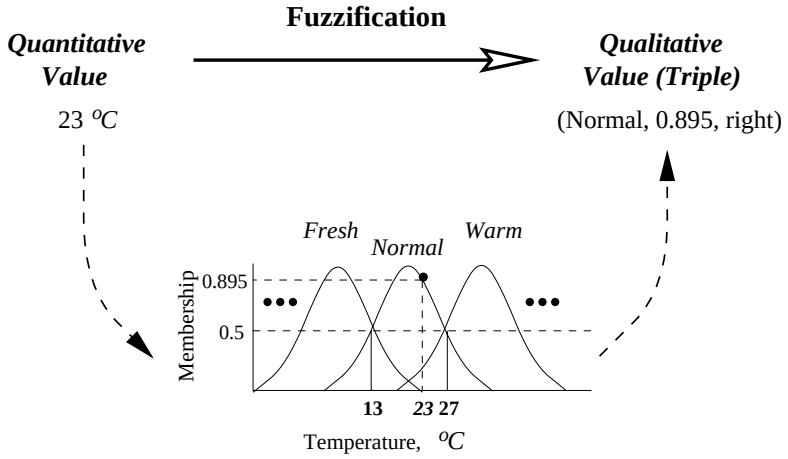

Figure 12. Fuzzy inductive reasoning (FIR) fuzzification of a temperature value of 23°C

the resulting state transition matrices as deterministic as possible. If such a relationship is found for every output variable, the behavior of the system can be forecast by iterating through the state transition matrices. The more deterministic the state transition matrices, the higher the likelihood that the future system behavior will be predicted correctly.

A possible relation among the qualitative variables of a five-variable system example could be of the following form:

$$y_1(t) = \tilde{f}(y_3(t - 2\delta t), u_2(t - \delta t), y_1(t - \delta t), u_1(t)), \tag{18}$$

where $\tilde{f}$ denotes a qualitative relationship. Notice that $\tilde{f}$ does not stand for any (known or unknown) explicit formula relating the input arguments to the output argument but only represents a generic causality relationship that, in the case of the FIR methodology, will be encoded in the form of a tabulation of likely behavior patterns (i.e., a state transition matrix).

In FIR, equation (18) is represented by the following so-called "mask" matrix:

$$\begin{array}{c} t \backslash x \\ t - 2\delta t \\ t - \delta t \\ t \end{array} \begin{array}{c} \begin{array}{ccccc} u_1 & u_2 & y_1 & y_2 & y_3 \end{array} \\ \begin{pmatrix} 0 & 0 & 0 & 0 & -1 \\ 0 & -2 & -3 & 0 & 0 \\ -4 & 0 & +1 & 0 & 0 \end{pmatrix} \end{array}. \tag{19}$$

The negative elements in this matrix are referred to as m-inputs, which denote input arguments of the qualitative functional relationship. They can be either inputs or outputs of the subsystem to be modeled, and they can have different time stamps. The above example contains four m-inputs. The sequence in which they are enumerated is immaterial. They are usually enumerated from left to right and top to bottom. The single positive value denotes the m-output. The terms *m-input* and *m-output* are used to avoid potential confusion with the inputs and outputs of the system. In the above example, the first m-input, i_1, corresponds to the output variable y_3 two sampling intervals back, $y_3(t - 2\delta t)$, whereas the second m-input refers to the input variable u_2 one sampling interval into the past, $u_2(t - \delta t)$, and so forth.

In the FIR methodology, such a representation is called a *mask*. A mask denotes a dynamic relationship among qualitative variables. A mask has the same number of columns as the qualitative behavior to which it should be applied, and it has a certain number of rows, the *depth* of the mask. The mask can be used to "flatten" dynamic relationships into "pseudo-static" relationships. This process is illustrated in Figure 13. The left-hand side of Figure 13 shows an excerpt of the *class value matrix*, one of the three matrices belonging to the *qualitative data model*. It shows the numerical rather than the symbolic class values. In the example shown in Figure 13, the first and second variables, u_1 and u_2, were discretized into two classes, whereas the remaining variables—y_1, y_2, and y_3—have been discretized into three classes each. The dashed box symbolizes the mask that is shifted downwards along the class value matrix. The round shaded "holes" in the mask denote the positions of the m-inputs, whereas the square shaded "hole" indicates the position of the m-output. The class values are read out from the class value matrix through the "holes" of the mask and are placed next to each other in the *behavior matrix* that is shown on the right-hand side of Figure 13. Here, each row represents one position of the mask along the class value matrix. It is lined up with the bottom row of the mask. Each row of the behavior matrix represents one pseudo-static qualitative state or qualitative rule. For example, the shaded rule of Figure 13 can be read as follows: If the first m-input, i_1, has a value of 2 (corresponding to "medium"); the second m-input, i_2, has a value of 1 (corresponding to "low"); the third m-input, i_3, has a value of 2 (corresponding to "medium"); and the fourth m-input, i_4, has a value of 2 (here corresponding to "high"), then

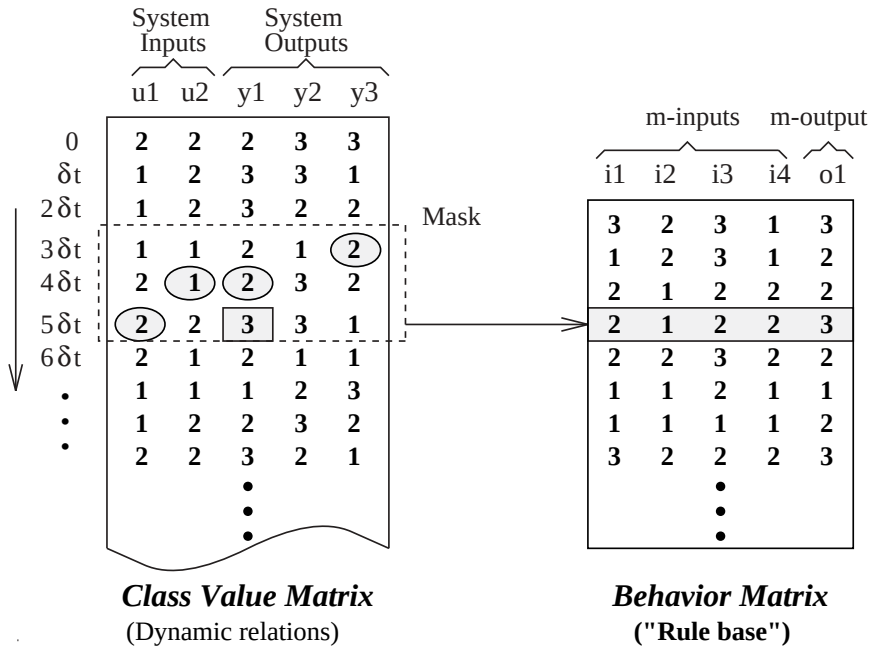

Figure 13. Process of flattening dynamic relationships into pseudo- static relationships using a mask

the m-output, o_1, assumes a value of 3 (corresponding to "high").

The qualitative rules can be invoked during qualitative simulation to predict new qualitative outputs. Clearly, these rules can be written in any order (i.e., the sequencing of the rows of the behavior matrix has become irrelevant). They can be sorted alphanumerically. The sorted behavior matrix is called the *state transition matrix*.

From the way in which the state transition matrix is constructed, it is clear that the same input pattern, a so-called *input state*, can be associated with different output values (i.e., a different *output state*). If the relationship between input states and output states is nondeterministic, there will be uncertainty associated with predictions made. Thus, it is advantageous to make the state transition matrix as deterministic as possible.

How is a mask found that, within the framework of all allowable masks, represents the most deterministic state transition matrix (i.e., optimizes the predictiveness of the model)? In FIR, the concept of a *mask candidate matrix* has been introduced. A mask candidate matrix is an ensemble of all possible masks from which the best is chosen by either a mechanism of an exhaustive search of exponential complexity or by one of various suboptimal search strategies of polynomial complexity, as described in Nebot and Jerez [18] and Jerez and Nebot [19]. The mask candidate matrix contains -1 elements where the mask has a potential m-input, a $+1$ element where the mask has its m-output, and 0 elements to denote forbidden connections. Thus, a good mask candidate matrix to determine a predictive model for variable y_1 in a five-variable system example might be the following:

$$\begin{array}{c} {}_t\backslash^x \\ t-2\delta t \\ t-\delta t \\ t \end{array} \begin{array}{c} \begin{array}{ccccc} u_1 & u_2 & y_1 & y_2 & y_3 \end{array} \\ \begin{pmatrix} -1 & -1 & -1 & -1 & -1 \\ -1 & -1 & -1 & -1 & -1 \\ -1 & -1 & +1 & 0 & 0 \end{pmatrix} \end{array}. \tag{20}$$

Corresponding mask candidate matrices are used to find predictive models for y_2 and y_3.

Each of the possible masks is compared to the others with respect to its potential merit (i.e., the degree of determinism associated with the state transition matrix constructed from it). The optimality of the mask is evaluated with respect to the maximization of its forecasting power.

The *Shannon entropy measure* is used to determine the *uncertainty* associated with forecasting a particular output state given any legal input state. The Shannon entropy relative to one input state is calculated from the following equation:

$$H_i = \sum_{\forall o} \mathrm{p}(o|i) \cdot \log_2 \mathrm{p}(o|i), \tag{21}$$

where $\mathrm{p}(o|i)$ is the "conditional probability" of a certain m-output state o to occur, given that the m-input state i has already occurred. The term *probability* is meant in a statistical rather than in a true probabilistic sense. It denotes the quotient of the observed frequency of a particular state divided by the highest possible frequency of that state.

The overall entropy of the mask is then computed as the following sum:

$$H_m = -\sum_{\forall i} \mathrm{p}(i) \cdot H_i, \tag{22}$$

where $\mathrm{p}(i)$ is the probability of that input state to occur. The highest possible entropy $H_{\max}$ is obtained when all probabilities are equal, and a zero entropy is encountered for relationships that are totally deterministic.

A normalized overall entropy reduction H_r is defined as

$$H_r = 1.0 - \frac{H_m}{H_{\max}}. \tag{23}$$

H_r is obviously a real-valued number in the range between 0.0 and 1.0, where higher values usually indicate an improved forecasting power. The masks with highest entropy reduction values generate forecasts with the smallest amounts of uncertainty.

One problem still remains. The size of the behavior matrix increases as the complexity of the mask grows; consequently, the number of legal states of the model grows quickly. Since the total number of observed data records remains constant, the frequency of observation of each state shrinks rapidly, and so does the predictiveness of the model. The entropy reduction measure does not account for this problem. With increasing complexity, H_r simply keeps growing. Very soon, a situation is encountered where every state that has ever been observed has been observed precisely once. This obviously leads to a totally deterministic state transition matrix, and H_r assumes a value of 1.0. Yet the predictiveness of the model will be dismal since, in all likelihood, already the next predicted state has never before been observed, and that means the end of forecasting. Therefore, this consideration must be included in the overall quality measure.

From a statistical point of view, every state should be observed at least five times [20]. Therefore, an *observation ratio*, O_r, is introduced as an additional contributor to the overall quality measure:

$$O_r = \frac{5 \cdot n_{5\times} + 4 \cdot n_{4\times} + 3 \cdot n_{3\times} + 2 \cdot n_{2\times} + n_{1\times}}{5 \cdot n_{\mathrm{leg}}}, \tag{24}$$

where

n_{leg} = number of legal m-input states,
$n_{1\times}$ = number of m-input states observed only once,
$n_{2\times}$ = number of m-input states observed twice,
$n_{3\times}$ = number of m-input states observed thrice,
$n_{4\times}$ = number of m-input states observed four times,
$n_{5\times}$ = number of m-input states observed five times or more.

If every legal m-input state has been observed at least five times, O_r is equal to 1.0. If no m-input state has been observed at all (no data are available), O_r is equal to 0.0. Thus, O_r can also be used as a quality measure.

The overall *quality of a mask*, Q_m, is then defined as the product of its uncertainty reduction measure, H_r, and its observation ratio, O_r:

$$Q_m = H_r \cdot O_r. \tag{25}$$

The *optimal mask* is the mask with the largest Q_m value.

8.4 Qualitative Simulation

Once the best model is obtained by means of computing the quality measure presented above, future output states can be predicted using the inference engine that is at the heart of the qualitative simulation module inside the FIR. The prediction procedure is presented in the diagram of Figure 14. The mask is placed on top of the qualitative data matrix in such a way that the m-output matches with the first element to be predicted. The values of the m-inputs are read out from the mask, and the behavior matrix (rule base) is used to determine the future value of the m-output, which can then be copied back into the qualitative data matrix. The mask is then shifted further down one position to predict the next output value. This process is repeated until all the desired values have been forecast. The qualitative simulation process predicts an entire qualitative triple from which a quantitative variable can be obtained whenever needed.

Using the 5-NN fuzzy inferencing algorithm, the membership and side functions of the new input are compared with those of all previous recordings of the same qualitative input. The input with the most similar membership and side functions is identified. For this purpose, a normalized defuzzification,

$$pos_i = class_i + side_i \cdot (1.0 - Memb_i), \tag{26}$$

is computed for every input variable of the new input set, and these pos_i values are stored in a vector, **pos**. The index i represents the ith input variable in the input state of the current observation. $Memb_i$ is the membership value, and $class_i$ and $side_i$ are the numeric class and side values associated with those inputs, respectively. The position value, pos_i, can be interpreted as a normalized defuzzification of the ith input variable. Irrespective of the original values of the input variable, pos_i assumes values in the range [1.0, 1.5] for the lowest class, [1.5, 2.5] for the next higher class, and so forth.

The defuzzification is repeated for all previous recordings of the same input state:

$$pos_{ij} = class_{ij} + side_{ij} \cdot (1.0 - Memb_{ij}), \tag{27}$$

where the index j denotes the jth previous observation of the same input state. Also, the pos_{ij} values are stored in a vector, $\mathbf{pos_j}$. Then, the $\mathcal{L}_2$ norms of the difference between the **pos** vector of the new input state and the $\mathbf{pos_j}$

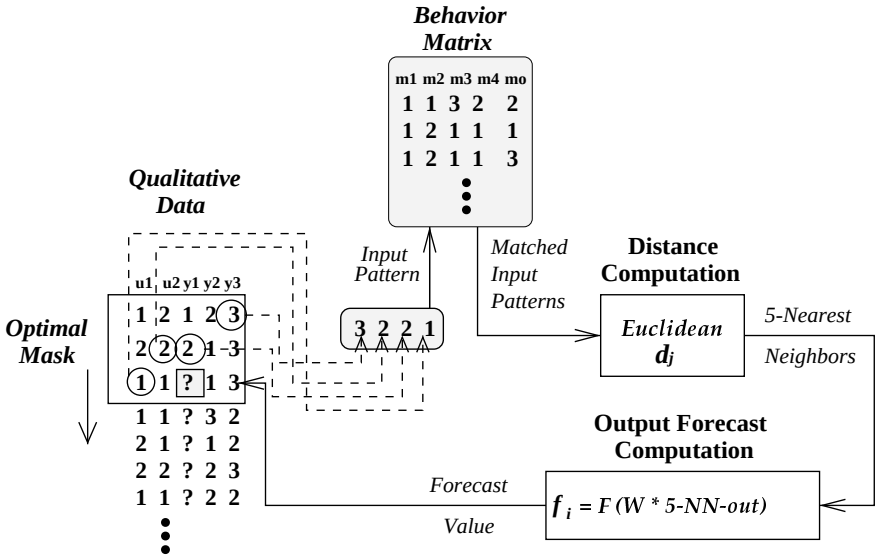

Figure 14. Qualitative simulation process diagram

vectors of all previous recordings of the same input state are computed:

$$dis_j = \sqrt{\sum_{i=1}^{N}(pos_i - pos_{ij})^2}, \tag{28}$$

where N is the number of m-inputs.

Finally, the previous recording with the smallest $\mathcal{L}_2$ norm is identified. The *class* and *side* values of the output state associated with this input state are then used as forecasts for the *class* and *side* values of the new output state.

Forecasting of the new membership function is done a little differently. Here, the five previous recordings with the smallest $\mathcal{L}_2$ norms are used (if at least five such recordings are found in the behavior matrix), and a distance-weighted average of their fuzzy membership functions is computed and used as the forecast for the fuzzy membership function of the current state. This is done in the following way.

The distances of each of the five nearest neighbors are limited from below by ϵ, the smallest number that is distinguishable from 1.0; in addition,

$$d_j = \max([dis_j, \epsilon]). \tag{29}$$

s_d is the sum of all d_j values:

$$s_d = \sum_{j=1}^{5} d_j. \tag{30}$$

Relative distances are then computed as

$$d_{\mathrm{rel}_j} = \frac{d_j}{s_d}. \tag{31}$$

Absolute weights are then computed as follows:

$$w_{\mathrm{abs}_j} = \frac{1.0}{d_{\mathrm{rel}_j}}. \tag{32}$$

Using the sum of the absolute weights,

$$s_w = \sum_{j=1}^{5} w_{\mathrm{abs}_j}, \tag{33}$$

it is possible to compute relative weights,

$$w_{\mathrm{rel}_j} = \frac{w_{\mathrm{abs}_j}}{s_w}. \tag{34}$$

The relative weights are numbers between 0.0 and 1.0. Their sum is always equal to 1.0. It is therefore possible to interpret the relative weights as percentages. Using this idea, the membership function of the new output can be computed as a weighted sum of the membership functions of the outputs of the previously observed five nearest neighbors:

$$Memb_{\mathrm{out}_{\mathrm{new}}} = \sum_{j=1}^{5} w_{\mathrm{rel}_j} \cdot Memb_{\mathrm{out}_j}. \tag{35}$$

8.5 Defuzzification

The defuzzification process of the FIR methodology is responsible for converting each qualitative-predicted output triple back to a quantitative output value. It is the inverse operation of the previously described fuzzification engine. Since the qualitative triples retain complete knowledge of the quantitative variables they represent, the defuzzification operation is unambiguous, as long as no fuzzy membership functions with horizontal flat roofs, such as trapezoidally shaped fuzzy membership functions, are being used.

9. Acknowledgments

We wish to thank Dr. Julio J. Valdés of the National Research Council of Canada for his suggestions related to the use of Markovian models. The research presented in this study has been financially supported by the Consejo Interministerial de Ciencia y Tecnología (CICYT), under project DPI2002-03225.

10. References

[1] Beneken, J., and V. Rideout. 1968. The use of multiple models in cardiovascular system studies: Transport and perturbation methods. *IEEE Transactions on Biomedical Engineering* BME-15-4:281-9.

[2] Snyder, M., and V. Rideout. 1969. Computer simulation studies of the venous circulation. *IEEE Transactions on Biomedical Engineering* 17:207-11.

[3] Sagawa, K., L. Maughan, H. Suga, and K. Sunagawa. 1988. *Cardiac contraction and the pressure-volume relationship*. New York: Oxford University Press.

[4] Vallverdú, M., C. Crexells, and P. Caminal. 1994. Cardiovascular responses to intrathoracic pressure variations in coronary disease patients: A computer simulation. *Technology in Health Care* 2:119-40.

[5] Nebot, A., F. Cellier, and M. Vallverdú. 1998. Mixed quantitative/qualitative modeling and simulation of the cardiovascular system. *Computer Methods and Programs in Biomedicine* 55:127-55.

[6] Cueva, J., R. Alquezar, and A. Nebot. 1997. Experimental comparison of fuzzy and neural network techniques in learning models of the central nervous system control. In *Proceedings EUFIT'97, 5th European Congress on Intelligent Techniques and Soft Computing*, September, Aachen, Germany, pp. 1014-8.

[7] Vallverdú, M. 1993. Modelado y Simulación del Sistema de Control Cardiovascular en Pacientes con Lesiones Coronarias. Ph.D. diss., Institut de Cibernètica, Universitat Politècnica de Catalunya.

[8] Suga, H., and K. Sagawa. 1974. Instantaneous pressure-volume relationships and their ratio in the excised, supported canine left ventricle. *Circulation Research* 53:117-26.

[9] Leaning, M., H. Pullen, E. Carson, and L. Finkelstein. 1983. Modelling a complex biological system: The human cardiovascular system. *Transactions on Instrumentation, Measurement, and Control* 5:71-86.

[10] Hyndman, P. 1970. A digital simulation of the human cardiovascular system and its use in the study if sinus arrhythmia. Ph.D. diss., Imperial College, University of London.

[11] Katona, P., O. Barnet, and W. Jackson. 1967. Computer simulation of the blood pressure control of the heart period. *Baroreceptors and Hypertension*, 191-9.

[12] Klir, G. 1969. *An Approach to general system theory*. New York: Van Nostrand Reinhold.

[13] Nebot, A., F. Cellier, and D. Linkens. 1996. Synthesis of an anaesthetic agent administration system using fuzzy inductive reasoning. *Artificial Intelligence in Medicine* 8 (3): 147-66.

[14] Nebot, A., M. Medina, and F. Cellier. 1994. The causality horizon: Limitations to predictability of behavior using fuzzy inductive reasoning. In *Proceedings ESM'94, European Simulation Multiconference*, June, Barcelona, Spain, pp. 492-6.

[15] Alquezar, R., J. Cueva, J. Valdés, A. Nebot, and P. Caminal. 1998. Learning a multi-subject model of the central nervous system control using neural networks. In *Proceedings EIS'98, International Symposium on Engineering of Intelligent Systems*, February, Tenerife, Spain, pp. 206-12.

[16] MGA Software. 1995. *Advanced continuous simulation language (ACSL)*. Reference manual. Version 11. Concord, MA: MGA Software.

[17] The MathWorks, Inc. 1993. *MATLAB: High-performance numeric computation and visualization software: User's guide*. Natick, MA: The MathWorks, Inc.

[18] Nebot, A., and T. Jerez. 1997. Assessment of classical search techniques for identification of fuzzy models. In *Proceedings EUFIT'97, 5th European Congress on Intelligent Techniques and Soft Computing*, September, Aachen, Germany, pp. 904-9.

[19] Jerez, T., and A. Nebot. 1997. Genetic algorithms vs. classical search techniques for identification of fuzzy models. In *Proceedings EUFIT'97, 5th European Congress on Intelligent Techniques and Soft Computing*, September, Aachen, Germany, pp. 769-73.

[20] Law, A., and W. Kelton. 1991. *Simulation modeling and analysis*. 2d ed. New York: McGraw-Hill.

Angela Nebot *is an associate professor at Llenguatges i Sistemes Informàtics, Universitat Politècnica de Catalunya, Barcelona, Spain.*

Francisco Mugica *is a researcher at Centro de Inv. en Ciencia Aplicada y Tec. Avanzada (CICATA), Instituto Politécnico Nacional, Mexico.*

François E. Cellier *is a professor in the Department of Electrical and Computer Engineering, University of Arizona, Tucson.*

Montserrat Vallverdú *is a researcher in the Dept. ESAII—Centre de Recerca en Eng. Biomèdica, Universitat Politècnica de Catalunya, Barcelona, Spain.*